Proceedings of ALGORITMY 2009
pp. 304–312

APPLICATION OF DISCONTINUOUS GALERKIN METHOD FOR THE SIMULATION OF 3D INVISCID COMPRESSIBLE FLOWS *

M. HOLÍK

Abstract. We deal with the numerical solution of the Euler equations in three dimensions. We define the problem and propose a numerical method for its solution. Finaly, we employ a combination of the discontinuous Galerkin finite element method and backward difference formulae. Due to a linearization and a suitable explicit extrapolation we solve only a system of linear algebraic equations at each time step. This leads us to an efficient numerical scheme which has a higher degree of approximation with respect to the space and time coordinates. The determination of these semi–implicit schemes is briefly described. The three dimensional stabilization technique and the new method to choice the time step are developed and some numerical examples are presented.

Key words. discontinuous Galerkin method, compressible flow, stabilization

AMS subject classifications. 65N30, 65N50

1. Introduction. Our goal is to solve an unsteady inviscid compressible flow which is described by the system of the *Euler equations*. Our aim is to develop a sufficiently efficient, robust and accurate numerical method for solving various problems in engineering.

It is promising to use the *discontinuous Galerkin method* (DGM), which is based on a piecewise polynomial but discontinuous approximation, which is suitable for problems with discontinuities, see [1], [2], [3], [4], [5], [6], [7] or [8].

The most usual approach for the time discretization is method of lines. Explicit methods such as the Runge-Kutta methods are very popular for their simplicity and a high order of accuracy. However, they suffer from a strong restriction of the time step. On the other hand fully implicit schemes lead to a system of highly nonlinear algebraic equations at each time step whose solution is complicated. To avoid this disadvantage we employ a semi-implicit method for the time discretization, which is based on a suitable linearization of the fluxes. The linear terms are treated implicitly and nonlinear ones explicitly. Advantage of this procedure is that we need to solve only linear algebraic problem in each time step, see [6], [7] or [8]. Within this paper we extend this results from two dimensional problem to three dimensions. Moreover we extend the stabilization techinque from [9] to three dimensions and present a new strategy for the choice of the time step.

2. Compressible flow problem. For the description of motion of an inviscid compressible flow we use the system of Euler equations.

Let $\Omega \subset \mathbb{R}^3$ be a bounded domain and $T > 0$. We set $Q_T = \Omega \times (0, T)$ and by $\partial\Omega$ we denote the boundary of Ω which consists of several disjoint parts. We distinguish inlet Γ_I, outlet Γ_O and impermeable walls Γ_W on $\partial\Omega$. The Euler equations can be written in the dimensionless form.

$$\frac{\partial \boldsymbol{w}}{\partial t} + \nabla \cdot \vec{f}(\boldsymbol{w}) = 0 \quad \text{in } Q_T, \tag{1}$$

*This work is a part of the research project MSM 0021620839 financed by the Ministry of Education of the Czech Republic and was partly supported by the Grant No. 316/2006/B-MAT/MFF of the Grant Agency of the Charles University Prague. Additionally, this work is a part of the research project ADIGMA, No. 30719 financed within the 3^{rd} Call of the 6^{th} European Framework Programe.

where

$$\boldsymbol{w} = (w_1, \dots, w_5)^{\mathrm{T}} = (\rho,\, \rho v_1,\, \rho v_2, \rho v_3,\, e)^{\mathrm{T}} \tag{2}$$

is the so-called *state vector* and $\vec{f} = (\boldsymbol{f}_1, \dots, \boldsymbol{f}_3)$

$$\begin{aligned}\boldsymbol{f}_s(\boldsymbol{w}) &= (f_s^{(1)}(\boldsymbol{w}), \dots, f_s^{(5)}(\boldsymbol{w}))^{\mathrm{T}} \\ &= (\rho v_s,\, \rho v_s v_1 + \delta_{s1} p,\, \rho v_s v_2 + \delta_{s2} p,\, \rho v_s v_3 + \delta_{s3} p,\, (e+p)\, v_s)^{\mathrm{T}},\ s = 1,2,3\end{aligned} \tag{3}$$

are the so-called *inviscid (Euler) fluxes*, where ρ – density, $\boldsymbol{v} = (v_1, v_2, v_3)$ – velocity, p – pressure, e – total energy and δ_{sk} is Kronecker's delta(if $s = k$, then $\delta_{sk} = 1$, else $\delta_{sk} = 0$).

In order to close the system we use the *state equation for perfect gas*

$$p = (\gamma - 1)\,(e - \rho|\boldsymbol{v}|^2/2), \tag{4}$$

where γ is the Poisson adiabatic constant. The system (1) - (4) is of *hyperbolic* type. It is equipped with initial condition

$$\boldsymbol{w}(x, 0) = \boldsymbol{w}^0(x), x \in \Omega, \tag{5}$$

and boundary conditions

$$B(\boldsymbol{w}) = 0 \text{ on } \partial\Omega \times (0, T). \tag{6}$$

Let $\partial\Omega$ is formed by disjoint part of Γ_{IO} and Γ_W representing the inflow/outflow and impermeable walls, respectively. On Γ_W we prescribe the impermeability condition

$$\boldsymbol{v} \cdot \boldsymbol{n} = 0 \text{ on } \Gamma_W, \tag{7}$$

where $\boldsymbol{v}$ denotes velocity and $\boldsymbol{n}$ the unit outer normal to $\partial\Omega$. On Γ_{IO} we prescribe m_n quantities of state vector $\boldsymbol{w}$ from dirichlet boundary condition, where m_n is number of negative eigenvalues of the matrix

$$\boldsymbol{P}(\boldsymbol{w}, \boldsymbol{n}) := \sum_{s=1}^{3} \boldsymbol{A}_s(\boldsymbol{w}) n_s, \tag{8}$$

where $\boldsymbol{A}_s$ are jacobi matrices of the mappings $\boldsymbol{f}_s$ from (3) and extrapolete m_p quantities of $\boldsymbol{w}$ from interior of Ω, where $m_p = 5 - m_n$, see [6].

3. Discretization. For discretization we employ the *discontinuous Galerkin finite element method* (DGFEM), which takes advantages from finite element method as well as from finite volume method. DGFEM is based on piecewise polynomial approximation without any requirement on interelement continuity what is suitable for problems where shock waves and contact discontinuities appear.

Let $\mathcal{T}_h$ ($h > 0$) be a partition of the domain Ω into a finite number of closed 3-dimensional mutually disjoint simplexes and/or parallelograms K i.e., $\overline{\Omega} = \bigcup_{K \in \mathcal{T}_h} K$. We call $\mathcal{T}_h = \{K\}_{K \in \mathcal{T}_h}$ a *triangulation* of Ω and do not require the conforming properties from the finite element method. We define the set of all faces $\mathcal{F}_h$ and the set of all inner faces $\mathcal{F}_h^I$ and a unit normal vector $\boldsymbol{n}_\Gamma$ as can be seen in [10].

Over the triangulation $\mathcal{T}_h$ we define the *broken Sobolev space*

$$H^k(\Omega, \mathcal{T}_h) = \{v; v|_K \in H^k(K)\ \forall\, K \in \mathcal{T}_h\}, \tag{9}$$

where $H^k(K) = W^{k,2}(K)$ denotes the (classical) Sobolev space on element K.

For each $\Gamma \in \mathcal{F}_h^I$ there exist two elements $K_p, K_n \in \mathcal{T}_h$ such that $\Gamma \subset K_p \cap K_n$. We use a convention that K_n lies in the direction of $\boldsymbol{n}_\Gamma$ and for $v \in H^1(\Omega, \mathcal{T}_h)$, we introduce the following notation:

$$
\begin{aligned}
v|_\Gamma^{(p)} &\equiv \text{the trace of } v|_{K_p} \text{ on } \Gamma, \\
v|_\Gamma^{(n)} &\equiv \text{the trace of } v|_{K_n} \text{ on } \Gamma, \\
[v]_\Gamma &\equiv v|_\Gamma^{(p)} - v|_\Gamma^{(n)}.
\end{aligned} \tag{10}
$$

For boundary faces $\Gamma \in \partial\Omega$ there exists element $K_p \in \mathcal{T}_h$ such that $\Gamma \subset \overline{K}_p \cap \partial\Omega$. Then for $v \in H^1(\Omega, \mathcal{T}_h)$, we introduce the following notation:

$$
\begin{aligned}
v|_\Gamma^{(p)} &\equiv \text{the trace of } v|_{K_p} \text{ on } \Gamma, \\
\langle v \rangle_\Gamma &\equiv [v]_\Gamma \equiv v|_\Gamma^{(p)} \equiv v|_\Gamma^{(n)}.
\end{aligned} \tag{11}
$$

Similarly as in [10] for $\boldsymbol{w}, \boldsymbol{\varphi} \in \left[H^2(\Omega, \mathcal{T}_h)\right]^5$, we define the forms:

$$
(\boldsymbol{w}, \boldsymbol{\varphi}) = \sum_{K \in \mathcal{T}_h} \int_K \boldsymbol{w} \cdot \boldsymbol{\varphi} \, \mathrm{d}x \tag{12}
$$

L^2 scalar product and

$$
\begin{aligned}
\bar{\boldsymbol{b}}_h(\boldsymbol{w}, \boldsymbol{\varphi}) = &- \sum_{K \in \mathcal{T}_h} \int_K \sum_{s=1}^{3} \boldsymbol{f}_s(\boldsymbol{w}) \cdot \frac{\partial \boldsymbol{\varphi}}{\partial x_s} \, \mathrm{d}x \\
&+ \sum_{K \in \mathcal{T}_h} \int_{\partial K} \sum_{s=1}^{3} (\boldsymbol{f}_s(\boldsymbol{w})\, n_s) \cdot \boldsymbol{\varphi} \, \mathrm{d}S
\end{aligned} \tag{13}
$$

diffusive form.

Following the notation (12) - (13) we can present a weak formulation of Euler equation in the form:

$$
\frac{d}{dt}(\boldsymbol{w}(t), \boldsymbol{\varphi}) + \bar{\boldsymbol{b}}_h(\boldsymbol{w}(t), \boldsymbol{\varphi}) = 0, \quad \boldsymbol{w}(t), \boldsymbol{\varphi} \in H^2(\Omega, \mathcal{T}_h)^5, t \in (0, T), \tag{14}
$$

where $\boldsymbol{w}(t)$ denotes function on Ω such that $\boldsymbol{w}(t)(x) = \boldsymbol{w}(x,t), x \in \Omega$.

Now we shall introduce the space *semi–discretization*. The integrals over the faces in (13) are evaluated by the approach from the finite volume method. In the element K on the face Γ we use approximation

$$
\sum_{s=1}^{3} (\boldsymbol{f}_s(\boldsymbol{w}(t)) \cdot \boldsymbol{n}_\Gamma) \cdot \boldsymbol{\varphi}|_\Gamma \approx H\left(\boldsymbol{w}(t)|_\Gamma^{(\mathrm{in})}, \boldsymbol{w}(t)|_\Gamma^{(\mathrm{out})}, \boldsymbol{n}_\Gamma\right) \cdot \boldsymbol{\varphi}\Big|_\Gamma^{(\mathrm{in})}, \tag{15}
$$

where H is a *numerical flux*, $\boldsymbol{w}(t)|_\Gamma^{(\mathrm{in})}$ and $\boldsymbol{w}(t)|_\Gamma^{(\mathrm{out})}$ are values of $\boldsymbol{w}(t)$ on the face Γ from the interior and the exterior of element K, respectively, at the time t.

The approximate solution of problem (1) with initial and boundary condition is sought at each instant time t in the space of discontinuous piecewise polynomial functions $\boldsymbol{S}_h$ defined by

$$
\boldsymbol{S}_h \equiv [S_h]^5, \;\; S_h \equiv \{v; v|_K \in P^p(K) \; \forall \, K \in \mathcal{T}_h\}, \tag{16}
$$

where p is a positive integer and $P^p(K)$ denotes the space of all polynomials on K of degree $\le p$.

¿From the definition (13) using then notation (10) and the aproximation (15) we can define for $\boldsymbol{w}_h, \boldsymbol{\varphi}_h \in \boldsymbol{S}_h$ the form

$$\begin{aligned}\tilde{\boldsymbol{b}}_h(\boldsymbol{w}_h, \boldsymbol{\varphi}_h) = &- \sum_{K\in\mathcal{T}_h} \int_K \sum_{s=1}^{3} \boldsymbol{f}_s(\boldsymbol{w}_h(x)) \cdot \frac{\partial \boldsymbol{\varphi}_h(x)}{\partial x_s}\,\mathrm{d}x \\ &+ \sum_{\Gamma\in\mathcal{F}_h} \int_\Gamma H\left(\boldsymbol{w}_h|_\Gamma^{(\mathrm{in})}, \boldsymbol{w}_h|_\Gamma^{(\mathrm{out})}, \boldsymbol{n}_\Gamma\right)\cdot[\boldsymbol{\varphi}_h]\,\mathrm{d}S. \end{aligned} \tag{17}$$

In order to avoid the time step restriction and nonlinearity of the discretized problem, we carry out a linearization of the nonlinear form $\tilde{\boldsymbol{b}}_h$.

Now according to [6] we can define the form $\boldsymbol{b}_h(\bar{\boldsymbol{w}}_h, \boldsymbol{w}_h, \boldsymbol{\varphi}_h)$, which is linear with respect to the second and third argument and cosistent with $\tilde{\boldsymbol{b}}_h(\cdot,\cdot)$ by

$$\boldsymbol{b}_h(\boldsymbol{w}_h, \boldsymbol{w}_h, \boldsymbol{\varphi}_h) = \tilde{\boldsymbol{b}}_h(\boldsymbol{w}_h, \boldsymbol{\varphi}_h) \quad \forall\, \boldsymbol{w}_h, \boldsymbol{\varphi}_h \in \boldsymbol{S}_h. \tag{18}$$

For more details see, e.g. [6].

Now we introduce the full space-time discrete problem. The main idea of the semi-implicit discretization is to treat the linear parts of form $\boldsymbol{b}_h$ implicitly and their nonlinear parts explicitly. In order to obtain a sufficiently accurate approximation with respect to the time coordinate we use the so-called *backward difference formula* (BDF) for the solution of the ODE semidiscrete problem. Moreover, a suitable explicit higher order extrapolation is used in the nonlinear part of $\boldsymbol{b}_h$, see [8].

Let $0 = t_0 < t_1 < \ldots < t_r = T$ be a partition of $(0,T)$ and $\tau_k \equiv t_{k+1} - t_k,\ k = 0, 1, \ldots, r-1$.

Definition 3.1. *Functions $\boldsymbol{w}_h^{k+1},\ k = 0, \ldots, r-1$ are an approximate solution of problem (1) with some suitable initial and boundary conditions satisfying*

(a) $\boldsymbol{w}_h^{k+1} \in \boldsymbol{S}_h$,

(b)
$$\frac{1}{\tau_k}\left(\sum_{l=0}^{n} \alpha_l \boldsymbol{w}_h^{k+1-l}, \boldsymbol{\varphi}_h\right) + \boldsymbol{b}_h\left(\sum_{l=1}^{n} \beta_l \boldsymbol{w}_h^{k+1-l}, \boldsymbol{w}_h^{k+1}, \boldsymbol{\varphi}_h\right) = 0$$
$$\forall\, \boldsymbol{\varphi}_h \in \boldsymbol{S}_h,\ k = n-1, \ldots, r-1, \tag{19}$$

(c) $\boldsymbol{w}_h^0$ *is an* $\boldsymbol{S}_h$ *approximation of initial condition* $\boldsymbol{w}^0$,

(d) $\boldsymbol{w}_h^l \in \boldsymbol{S}_h,\ l = 1, \ldots, n-1$ *are given by a suitable one-step method,*

where $n \ge 1$ is the degree of the BDF scheme, the coefficients $\alpha_l,\ l = 0, \ldots, n$, and $\beta_l,\ l = 1, \ldots, n$, depend on time steps $\tau_{k-l},\ l = 0, \ldots, n$. The problem (19), (a) – (d) represents a system of linear algebraic equations for each $k = n-1, \ldots, r-1$, which is solved by a suitable iterative solver (e.g. GMRES method).

4. Stabilization. Application of this numerical scheme to transsonic flow leads to spurious overshoots and undershoots in computed quantities near shock waves. Therefore we use the stabilization of the scheme from [9], witch we generalize to three

dimensions. For each $K \in \mathcal{T}_h$ denote ∂K^I inner part of boundary of element K as $\partial K^I \equiv \partial K \setminus \partial\Omega$. According [9] we define the quantity

$$g_K^{2D}(\boldsymbol{w}_h) = \frac{\sum_{\Gamma\in\partial K^I}\int_\Gamma [\boldsymbol{w}_{h,1}]^2 ds}{|K|^{\frac{3}{4}}\sum_{\Gamma\in\partial K^I}|\Gamma|}, \tag{20}$$

that meassures the interelement jump of the first component of $\boldsymbol{w}_h$, what is piecewise polynomial aproximation of density function ρ. For this measure, we can also use another quantity such as pressure. For face we define $g_\Gamma^{2D}(\boldsymbol{w}_h)$ as aritmetical mean of $g_K^{2D}(\boldsymbol{w}_h)$ from adjacent elements. Moreover, we define the forms

$$d_h^{2D}(\boldsymbol{w}_h, \bar{\boldsymbol{w}}_h, \boldsymbol{\varphi}) = \sum_{K\in\mathcal{T}_h} h_K g_K^{2D}(\boldsymbol{w}_h)\int_K \nabla\bar{\boldsymbol{w}}_h\cdot\nabla\boldsymbol{\varphi}_h\,\mathrm{d}x, \tag{21}$$

where h_K is diameter of element K and

$$J_h^{2D}(\boldsymbol{w}_h, \bar{\boldsymbol{w}}_h, \boldsymbol{\varphi}) = \sum_{\Gamma\in K^I}\frac{g_\Gamma^{2D}(\boldsymbol{w}_h)}{|\Gamma|}\int_\Gamma [\bar{\boldsymbol{w}}_h][\boldsymbol{\varphi}_h]\,\mathrm{d}S \tag{22}$$

which represent so-called artifical viscosity and interior penalty, respectively. This desined stabilization for 2 dimensions from [9] is applied by adding term

$$d_h^{2D}(\boldsymbol{w}_h^k, \boldsymbol{w}_h^{k+1}, \boldsymbol{\varphi}) + J_h^{2D}(\boldsymbol{w}_h^k, \boldsymbol{w}_h^{k+1}, \boldsymbol{\varphi}) \tag{23}$$

to the left hand side of (19). Both terms are vanishing in region where $\boldsymbol{w}$ is smooth for $h \to 0$. The presented quantity (20) and forms (21) and (22) were derived for two dimensional computation in [9]. They are based on assumption that for smooth u is jump over face $[u]$ of order $O(h^{p+1})$, see [11], but in vicinity of discontinuity (shock wave) is $[u]$ order $O(1)$. Then quantity (20) is in region with smooth density $O(h^{2p+\frac{1}{2}})$ and $O(h^{-\frac{3}{2}})$ near the discontinuity. Moreover, the quantities (21) and (22) are order $O(h^{-\frac{1}{2}})$ and $O(h^{-\frac{3}{2}})$ in vicinity of discontinuity and $O(h^{2p+\frac{3}{2}})$ and $O(h^{2p+\frac{1}{2}})$ in other case, respectively.

We use the same idea in our three dimensional case. In quantity (20) we modify exponent of $|K|$ ($\frac{3}{4} \to \frac{1}{6}$) so that the new terms d_h^{3D} and J_h^{3D} will be of negative order in h in region near discontinuity and with maximal order in h in region with smooth solution. Hence we define quantity

$$g_K^{3D}(\boldsymbol{w}_h) = \frac{\sum_{\Gamma\in\partial K^I}\int_\Gamma [\boldsymbol{w}_{h,1}]^2 ds}{|K|^{\frac{1}{6}}\sum_{\Gamma\in\partial K^I}|\Gamma|}, \tag{24}$$

and the terms $J_h^{3D} \equiv J_h^{2D}$ given by (22) with term g_Γ^{3D} instead of g_Γ^{2D} and

$$d_h^{3D}(\boldsymbol{w}_h, \bar{\boldsymbol{w}}_h, \boldsymbol{\varphi}) = \sum_{K\in\mathcal{T}_h} g_K^{3D}(\boldsymbol{w}_h)\int_K \nabla\bar{\boldsymbol{w}}_h\cdot\nabla\boldsymbol{\varphi}_h\,\mathrm{d}x \tag{25}$$

which are of order $O(h^{2p+\frac{3}{2}})$ in smooth part of domain and $O(h^{-\frac{1}{2}})$ near discontinuity.

5. Adaptive time step. In order to achieve a steady-state solution in an efficient way it is necessary to adapt the time step during the computational process. In [12] , an adaptive choice of the time step based on a comparison of two BDF formulae was presented. Moreover we present an alternative heuristic choice of the time step

TABLE 1
Comparison of choice of time step for BDF from [8] and heuristic choice (HCh) from 26

method	DOF = 60 360 iter	CPU	DOF = 121 000 iter	CPU
BDF $tol = 10^{-2}$	64	275	74	1117
BDF $tol = 10^{-1}$	54	266	63	1042
HCh $\alpha = \frac{3}{2}$	39	177	59	863
HCh $\alpha = 2$	17	111	20	531

which is based on a idea to increase the time step when the "steady-state residuum" is decreasing. Hence we put $\tau_1 = \frac{CFL}{\Lambda_0}$ and:

$$\tau_{k+1} = \frac{CFL}{\Lambda_k}\left(\frac{\frac{1}{\tau_k}||\boldsymbol{w}_k - \boldsymbol{w}_{k-1}||}{\frac{1}{\tau_1}||\boldsymbol{w}_1 - \boldsymbol{w}_0||}\right)^{-\alpha}, \quad t = 1, 2, \ldots, \tag{26}$$

where

$$\Lambda_k = \max_{K\in\mathcal{T}_h} |K|^{-1} \max_{\Gamma\in\partial K} \max_{l=1,\ldots,5} \lambda_l(\boldsymbol{w}_h^k|_\Gamma)|\Gamma|.$$

This approach is motivated from explicit schemes where time step is bounded by the term $\frac{CFL}{\Lambda_k}$, where $CFL \in (0,1)$ is a suitable number, see [13]. Then $\tau_0 = \tau_1$ correspond to the size of the time step from explicit time discretization and for $k > 1$ τ_k is exponencially incerasingwhe steady state residuum $(= \frac{1}{\tau_k}||\boldsymbol{w}_k - \boldsymbol{w}_{k-1}||)$ is decreasing. Table 1 contains comparison of number of iteration and CPU time to reach steady state solution of the method based on two BDF formulae and our heuristic choice (26) with $CFL = \frac{1}{2}$ for two different computation with 60 360 and 121 000 degrees of freedom. Where *tol* is tolerance in BDF formulae, and α is coefficient in (26). We observe that the method of heuristic choice of time step (26) is faster adaptive method.

The presented numerical method is now being implemented within the object oriented patform COOLFluiD developed at the Von Karman Institute in Brussel, see [14].

6. Example. We present two examples Wedge3D and Jets3D of inviscid compressible flow with P1 DGFEM aproximation.

6.1. Wedge 3D. It is supersonic flow ($MACH = 2.0$) in channel forward facing oblique step, see Fig. 1. The initial condition is constant with values $\rho = 1.0, v = (2.366431913, 0.0, 0.0), e = 5.3$. Distribution of density in steady state sollution is in Fig. 2. This problem cannot be solved without stabilization and adaptive choice of time step greatly spare time of computation.

6.2. Jets 3D. It is flow in which computational domain is divided into two semi spaces with different initial state describing flow. To each domain flows from the boundary flow with same properties as is flow from initial condition, see Fig. 3. In Fig. 4 is disribution of density in case when as initial condition are chosen flows with $MACH$ 0.8 and 2.4. Most interesting is the case when as initial flows are chosen both supersonic flows with $MACH$ 4.0 and 2.4. The distribution of density is presented in Fig. 5. Due to adaptive choice of time step first case need only 15 and second case less than 35 iteration to reach steady state solution.

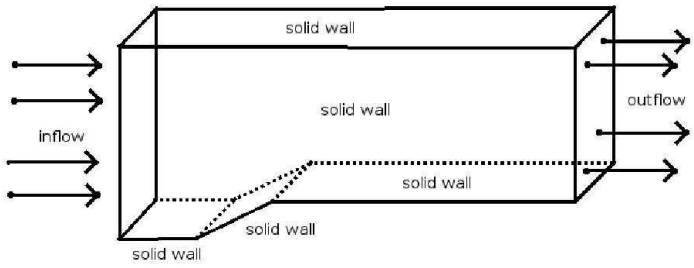

FIG. 1. *Description of WEDGE3D problem.*

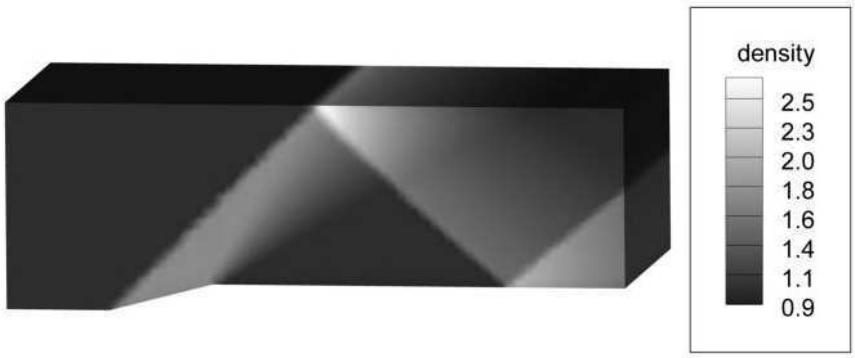

FIG. 2. *Distribution of density.*

7. Conclusion. We described a numerical solution of the Euler equations in three dimensions by a combination of DGFEM and BDF. We presented extension of the scheme to three dimensions, generalization of the stabilization technique and new choice of time step. Numerical examples demostrate a robustness of the proposed method.

We wish to express our sincere gratitude to Tiago Quintino (von Karman Institute, Belgium) for a large effort with an implementation of DGFEM scheme into COOLFLuiD platform.

REFERENCES

[1] F. Bassi and S. Rebay. High-order accurate discontinuous finite element solution of the 2D Euler equations. *J. Comput. Phys.*, 138:251–285, 1997.
[2] S. Rebay F. Bassi. A high order discontinuous galerkin method for compressible turbulent flow in: B. cockburn, g.e. karniadakis, c.-w. shu (eds.), discontinuous galerkin method: theory, computations and applications. *Computational Science and Engineering*, 11:113123, Springer, Berlin 2000.
[3] J.T. Oden C.E. Baumann. A discontinuous hp finite element method for the euler and navier-stokes equations. *Int. J. Numer. Meth. Fluids*, 31:7995, 1999.

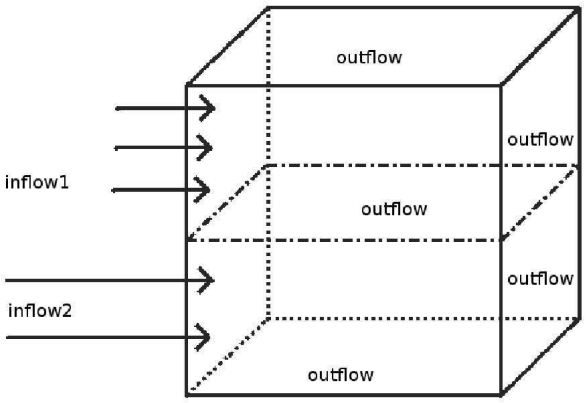

FIG. 3. *Description of JETS3D problem.*

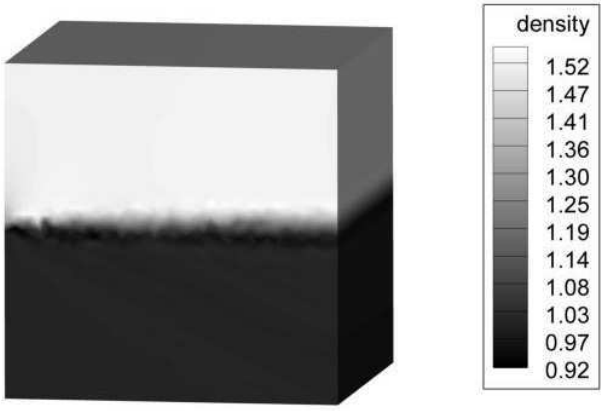

FIG. 4. *Distribution of density - MACH 0.8 and 2.4.*

[4] H. van der Ven J.J.W. van der Vegt. Space-time discontinuous galerkin finite element method with dynamic grid motion for inviscid compressible flow. *J. Comput. Phys.*, 182:546585, 2002.

[5] J.J.W. vander Vegt H. vander Ven. Space-time discontinuous galerkin finite element method with dynamic grid motion for inviscid compressible flows. ii. efficient flux quadrature. *Comput. Methods Appl. Mech. Engrg.*, 191:4747–4780, 2002.

[6] V. Dolejší and M. Feistauer. Semi-implicit discontinuous Galerkin finite element method for the numerical solution of inviscid compressible flow. *J. Comput. Phys.*, 198(2):727–746, 2004.

[7] M. Feistauer and V. Kučera. On a robust discontinuous galerkin technique for the solution of compressible flow. *J. Comput. Phys.*, 224(1):208–221, 2007.

[8] M. Feistauer, V. Dolejší, and V. Kučera. On the discontinuous Galerkin method for the simulation of compressible flow with wide range of mach numbers. *Comput Visual Sci*, 10:17–27, 2007.

[9] V. Dolejší. Discontinuous Galerkin method for the numerical simulation of unsteady compressible flow. *WSEAS Transactions on Systems*, 5(5):1083–1090, 2006.

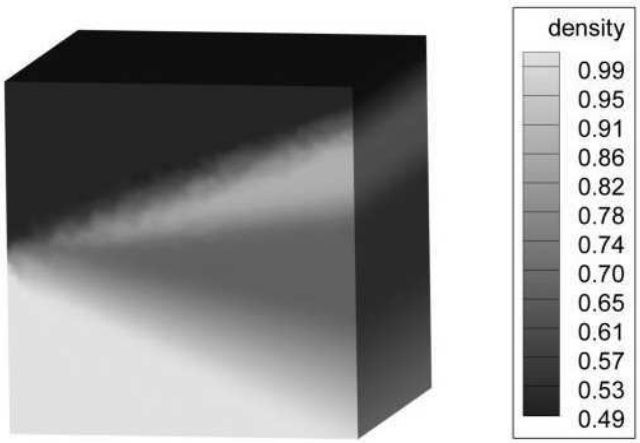

FIG. 5. *Distribution of density - MACH 4.0 and 2.4.*

[10] V. Dolejší. Semi-implicit interior penalty discontinuous Galerkin methods for viscous compressible flows. *Commun. Comput. Phys.*, 4(2):231–274, 2008.
[11] V. Dolejší, M. Feistauer, and C. Schwab. On some aspects of the discontinuous Galerkin finite element method for conservation laws. *Math. Comput. Simul.*, 61:333–346, 2003.
[12] V. Dolejší and P. Kůs. Adaptive backward difference formula – discontinuous Galerkin finite element method for the solution of conservation laws. *Int. J. Numer. Methods Eng.*, 73(12):1739–1766, 2008.
[13] Felcman J. Feistauer M. and Straškraba I. *Mathematical and Computational Methods for Compressible Flow.* Oxford University Press, Oxford, 2003.
[14] Home page of coolfluid : https://coolfluidsrv.vki.ac.be/coolfluid/.